Cite this: DOI: 10.1039/c0xx00000x

www.rsc.org/xxxxxx

ARTICLE TYPE

Discovery of a Silicon-based Ferrimagnetic Wheel Structure in $V_xSi_{12}^-$ (x = 1-3) Clusters: Photoelectron Spectroscopy and Density Functional Theory Investigation

Xiaoming Huang[1], Hong-Guang Xu[2], Shengjie Lu[2], Yan Su[1], R. B. King[4], Jijun Zhao*[1,3], and Weijun Zheng*[2]

Received (in XXX, XXX) Xth XXXXXXXXX 20XX, Accepted Xth XXXXXXXXX 20XX
DOI: 10.1039/b000000x

Our studies show that VSi_{12}^- adopts a V-centered hexagonal prism with a singlet spin state. Addition of the second V atom leads to a capped hexagonal antiprism for $V_2Si_{12}^-$ in a doublet spin state. Most interestingly, $V_3Si_{12}^-$ exhibits a ferrimagnetic bicapped hexagonal antiprism wheel-like structure with a total spin of 4 μ_B.

Silicon is the backbone of microelectronics industry. The miniaturization trend of electronic devices has motivated tremendous efforts to develop new silicon nanostructures[1] and to investigate silicon clusters [2-5]. Transition metal (TM) doped silicon clusters are of particular interest because the TM dopants not only can stabilize silicon clusters[6, 7] but also introduce novel physical/chemical properties such as large HOMO-LUMO gaps[8], high magnetic moments[9], and tunable hyperpolarizability[10]. Moreover, these metal-encapsulating silicon clusters may act as building blocks in novel materials[11, 12], such as one-dimensional (1D) ferromagnetic nanotubes[13-16].

Among the previous studies on the metal-doped silicon clusters, TM@Si_{12} clusters has attracted particular attention[6, 10, 14, 17-23]. Hiura et al.[6] reported high stability of a WSi_{12} cluster, which possesses an endohedral tungsten atom in a silicon cage configuration and fulfills the 18-electron rule.[24, 25] Sen and Mitas [26] systematically investigated encapsulation of a TM atom (3d, 4d, and 5d series) inside a Si_{12} hexagonal prism cage and found the cage configuration to be remarkably stable regardless of the species of TM atom. Khanna and co-workers[14] found that the stability of Cr@Si_{12} can be also explained by the 18-electron rule and the large magnetic moment (6 μ_B) of the Cr atom is completely quenched by the Si_{12} hexagonal prism. In addition, they also explored the ground state geometries, electronic properties, and stabilities of the other TM@Si_{12} (TM=Sc-Ni) clusters using density functional theory (DFT) calculations[17, 18].

Until now most experimental and theoretical studies are focused on silicon clusters doped with a single TM atom, while much less is known about silicon clusters with multiple TM dopants. Ji and Luo[27] investigated the geometries, magnetic properties and stabilities of a number of TM_2Si_{18} (TM = Ti, V, Cr, Mn, Fe, Co, Ni, Cu, Zn) clusters using DFT calculations. They found that the magnetic moments of these clusters are mostly quenched except that Mn_2Si_{18}, Fe_2Si_{18} and Cu_2Si_{18} are magnetic with total moments of 2 μ_B. A spin moment of 2 μ_B was also found in a hydrogenated $Cr_2Si_{18}H_{12}$ cluster [28]. Xu et al. used photoelectron spectroscopy and DFT to reveal strong V-V interaction and weak Sc-Sc interaction in the V_2Si_n[12, 29] and Sc_2Si_n[30] clusters, respectively. Furthermore, they showed that the V_2Si_{20} cluster has a V_2 unit encapsulated inside an elongated dodecahedron Si_{20} cage structure[12]. Since the V-V interaction is very strong, it would be especially interesting to investigate how the structures and properties of V-doped silicon clusters change upon incorporation of additional V atoms.

In this communication, we report photoelectron spectroscopy and density functional theory studies of $V_xSi_{12}^-$ (x=1, 2, 3) clusters illustrating the effect of multiple TM atoms on the equilibrium structures of silicon frameworks as well as the electronic and magnetic properties of the TM-Si binary clusters. Most impressively, we found that $V_3Si_{12}^-$ has a wheel- like bicapped hexagonal antiprism structure and is ferrimagnetic with a total magnetic moment of 4 μ_B, making it promising building block in nanoscale spintronics and high-density magnetic storage.

Table 1. Binding energy (E_b), VDE, ADE, and total magnetic moments of $V_xSi_{12}^-$ (x=1, 2, 3) clusters (unless specified with "Expt.", all values are from DFT calculations.

Cluster	E_b (eV/atom)	VDE (eV) Expt.	VDE (eV) Theo.	ADE (eV) Expt.	ADE (eV) Theo.	Spin (μ_B)
VSi_{12}^-	4.09	3.82±0.08	3.94	3.71±0.08	3.87	0
$V_2Si_{12}^-$	4.12	3.66±0.08	3.75	3.55±0.08	3.69	1
$V_3Si_{12}^-$	4.13	2.59±0.08	2.54	2.44±0.08	2.53	4

The lowest-energy configurations of $V_xSi_{12}^-$ (x=1, 2, 3) clusters from GA-DFT global optimizations are shown in Fig. 1. The structures of some low-lying isomers are given in Figure S1 of the Supporting Information. For each anionic cluster, we computed the vertical detachment energy (VDE) and adiabatic detachment energy (ADE). The binding energies, VDEs, ADEs, and total magnetic moments of these three clusters are summarized in Table 1. Based on the ground state geometries, the photoelectron spectra of $V_xSi_{12}^-$ (x=1, 2, 3) cluster anions are simulated using the PBE-DND scheme and compared with the experimental spectra in Fig. 2. The VDEs and ADEs from theoretical calculations are very close to the experimental values with average deviations of ~0.1 eV. The experimental photoelectron spectra of V_xSi_{12} cluster anions are also well reproduced by the theoretical calculations. The excellent agreements clearly indicate that our DFT-GA global search has located the true ground state configurations of the $V_xSi_{12}^-$ (x=1, 2, 3) clusters, and that our PBE/DND scheme is able to describe the electronic states of these clusters to a satisfactory extent.

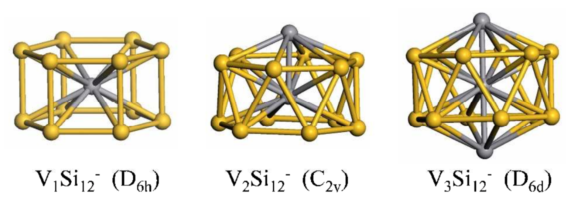

Fig. 1 Ground state structures of $V_xSi_{12}^-$ (x=1, 2, 3) clusters.

As shown in Fig. 1, VSi_{12}^- adopts a hexagonal prism cage (D_{6h}) with an endohedral V atom. This is in agreement with the structures of the neutral VSi_{12} [14, 26] and the VSi_{12}^- anion [18] found by previous DFT calculations as well as the distorted hexagonal prism structure of the VSi_{12}^+ cation found by infrared multiple photon dissociation spectroscopy[31]. Moreover, VSi_{12}^- possesses a closed shell electronic configuration with a large HOMO-LUMO gap of 2.01 eV, obeying the 18-electron rule[17, 18, 26]. Indeed, the spatial distributions of molecular orbitals exhibit the distinct feature of a $1S^21P^61D^{10}$ electron shell (Figure S2). Like its isoelectronic counterpart $CrSi_{12}$[17, 26], the VSi_{12}^- cluster is entirely non-magnetic. Previous DFT calculations[18, 26] predicted that the ground state of TM@Si_{12} clusters for the 3d TM series usually has the lowest spin multiplicity, i.e., singlet for even numbers of electrons and doublet for odd numbers of electrons.

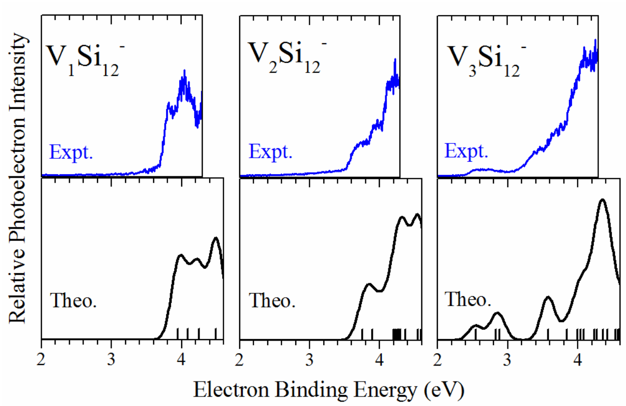

Fig. 2 Photoelectron spectra of $V_xSi_{12}^-$ (x=1, 2, 3) clusters. Upper: experiment, lower: theoretical simulation. In the theoretical spectra, a uniform Gaussian broadening of 0.1 eV is chosen and the energy levels of clusters from DFT calculations are labelled by short vertical lines.

Incorporation of another vanadium atom into VSi_{12}^- transforms the hexagonal prism cage of Si_{12} skeleton into a distorted Si_{12} hexagonal antiprism with C_{2v} symmetry, with the second V atom capping one of the hexagonal faces of the antiprism. Owing to the strong V-V interaction[12, 29], the two V atoms in $V_2Si_{12}^-$ cluster tend to stay together. Note that the isomer with two separated V atoms (isomer d in Figure S1) is energetically less favorable by 1.67 eV. Like VSi_{12}^-, $V_2Si_{12}^-$ still adopts the lowest spin multiplicity (doublet state).

Further addition of the third V atom leads to a bicapped hexagonal antiprism (D_{6d}). This can be viewed as a wheel structure, in which three V atoms form a central axle surrounded by the Si_{12} hexagonal antiprism. A similar D_{6h} wheel structure with a Si_{12} hexagonal prism rather than antiprism (isomer d in Figure S1) is found to be less stable by 0.912 eV. Clearly, incorporation of multiple V atoms has a pronounced effect on the geometry of Si_{12} frame. More impressively, the magnetism of V atoms are partially recovered after inclusion of the third V atom. According to our spin-polarized DFT calculations, doping three V atoms into Si_{12} cluster leads to a total magnetic moment of 4 μ_B for the anionic cluster and 3 μ_B for the neutral cluster, respectively.

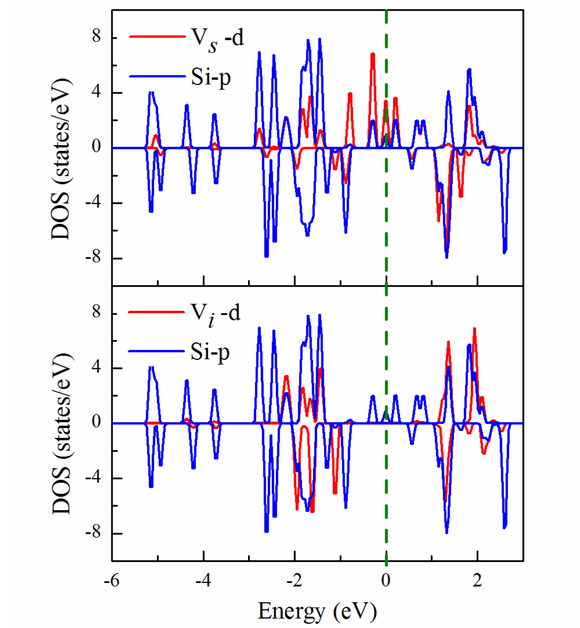

Fig. 3 Partial density of states (DOS) for $V_3Si_{12}^-$ cluster. Blue curves denote p orbitals of six Si atoms belonging to the same layer of the antiprism, and red curves are d orbitals of one V atom (upper for the surface V_s atom bonded with the six Si atoms, lower for the interior V_i atom). Green dashed line is the Fermi level.

The magnetic moments of the neutral and anionic V_3Si_{12} clusters can be interpreted by the Wade-Mingos rules[32, 33], which historically were derived to relate the structures of polyhedral boranes to the number of skeletal electrons. Later they were used to explain the shapes of other clusters isoelectronic and isolobal with boranes[34]. According to the Wade-Mingos rules, $2n$+2 electrons are needed for skeletal bonding in a deltahedron with n vertices where a deltahedron is defined as a polyhedron with all triangular faces. Normally counting skeletal electrons by the Wade-Mingos rules assumes that each vertex atom uses three valence orbitals for skeletal bonding, leaving any remaining orbitals for bonding to external groups or for lone pairs. In the case of V_3Si_{12}, the interior V atom contributes all of its five valence electrons, and the surface V atoms can be assumed to use a six-orbital sd^5 manifold since the 4p orbitals are too high in energy for its valence orbital manifold. This leaves three external orbitals to accommodate the five valence electrons of each surface V atom. One of these external orbitals thus has an unpaired electron thereby contributing to the overall spin of the cluster. As a consequence, the surface V atoms do not contribute any electrons to the skeletal bonding.

In counting skeletal electrons in V_3Si_{12}, each silicon atom contributes two skeletal electrons leaving an external lone pair. These two skeletal electrons for each silicon atom combined with the five skeletal electrons from the central vanadium atom leads to a total of 12×2+5=29 skeletal electrons corresponding to one hole, i. e., one unpaired electron in the 30 skeletal electron closed shell configuration for a 14-vertex bicapped square antiprism. This hole, together with the two unpaired electrons from the two surface vanadium atoms, result in a total of three unpaired electrons in the neutral V_3Si_{12}, corresponding to a magnetic moment of 3 μ_B. The extra electron in the $V_3Si_{12}^-$ anion does not pair up with any of these unpaired electrons, but instead increases the total magnetic moment to 4 μ_B.

Furthermore, population analysis of $V_3Si_{12}^-$ (Table S1) shows that the alignment of local magnetic moments on V atoms is ferrimagnetic with +2.4 μ_B on each of the surface V atoms and –0.6 μ_B on the interior V atom. The magnitude of on-site moment of the interior V atom is about 1/4 of that of surface V atom and non- negligible. There are also small and negligible induced moments on Si atoms (–0.018 μ_B on average). Intuitively, the ferrimagnetism of $V_3Si_{12}^-$ can be attributed to the different coordination numbers (CN) of the interior V atom (CN=14) and the surface V atoms (CN=7) as well as the different V-Si bond lengths, i.e., 2.682 Å for the interior V atom and 2.707 Å for the surface V atoms (Table S2). It is known that reduced CN and elongated interatomic distance can result in enhanced local magnetic moment on the TM atom in a cluster [35].

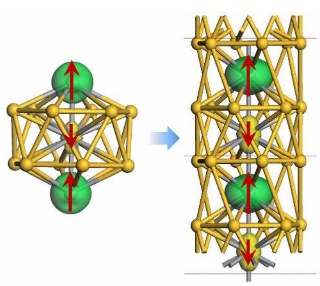

Fig. 4 Geometries and isosurfaces of spin densities (green for majority spin and yellow for minority spin) for $V_3Si_{12}^-$ cluster (left) and V_2Si_{12} nanowire (right).

The interactions between Si and V atoms can be further analyzed by the partial density of p and d states in Fig. 3 (contribution from s states is very little and thus not shown). It is known that p-d hybridization and Si-to-metal charge transfer are the two key factors for quench of local magnetic moment of TM atom in a metal doped silicon cluster [15, 16, 26]. From Fig. 3, one can see that the interior V atom has stronger p-d hybridization with surrounding Si atoms than the surface V atom. The local magnetic moment of +2.4 μ_B on each surface V atom mainly originates from the d states of the majority spin near Fermi level, which only hybridize little with the p states of Si atoms. On the other hand, the negative moment of –0.6 μ_B on the interior V atom can be related to the peak of d states of the minority spin located ~1 eV below the Fermi level, which does not overlap with the p states of Si atoms. On-site Mulliken population analysis (Table S1) also shows that the interior V atom gains 0.64 electrons from the surrounding Si atoms, while the surface V atom gains only about 0.09 electrons.

As shown in Fig. 4, the hexagonal antiprism of V_3Si_{12} may further act as building blocks for novel 1D V-centered Si nanowire, similar to the previous cases of TM@Si_{12} and TM@Si_{10} clusters [13-16]. Our spin-polarized DFT calculations show that the assembled nanowire is still ferrimagnetic, i.e., one V atom with spin moment of 1.076 μ_B, and another one with moment of –0.181μ_B. Previously, ferrimagnetic clusters were mainly observed in small transition metal oxide systems such as Fe_4O_6 [36], Mn_3O^-, $Mn_3O_2^-$, and Mn_4O^- [37]. Considering the advantage of the mature silicon-based microelectronic technology, the discovery of Si-based ferrimagnetic cluster (and possibly, 1D nanowire) is rather tempting for future spintronic applications [38], such as spin filter [39], exchange bias [40] and spin-resolved light-emitting diode (spin-LED) [41]. In the cluster assemblies, it might be possible to retain the negative charge on $V_3Si_{12}^-$ cluster by appropriately combining with elements of low electron affinity (e.g., alkali metals), like the cluster-assembled ionic solids of $K(Al_{13})$ [42] and $Cs(BAl_{12})$ [43].

To summarize, incorporation of more than one V atom in the Si_{12} host cluster not only modifies the equilibrium geometry but also partially recovers the magnetic moments of the V atoms. Combining anion photoelectron spectroscopy and DFT-based global search, $V_3Si_{12}^-$ cluster is shown to possess a bicapped hexagonal antiprism structure with ferrimagnetic alignment of local moments on the interior and surface V atoms. The Wade-Mingos rules is able to explain the four unpaired electrons in the 14-vertex deltahedron of $V_3Si_{12}^-$. The different local magnetic moments on V atoms are attributed to different p-d hybridizations between V and Si atoms. This ferrimagnetic $V_3Si_{12}^-$ (or V_3Si_{12}) cluster with high spin multiplicity is expected to be useful in future nanoscale magnetic materials and spintronic devices. Moreover, the present results suggest new opportunities in tailoring the electronic and magnetic properties of doped silicon clusters by varying the number and composition of transition metal dopants.

Methods

The experiments were conducted on a previously described[30] home-built apparatus consisting of a laser vaporization source, a time-of-flight (TOF) mass spectrometer, and a magnetic-bottle photoelectron spectrometer. The V-Si cluster anions were generated in the laser vaporization source by laser ablation of a rotating translating disk target (13 mm diameter, V/Si mole ratio 1:2) with a nanosecond Nd:YAG laser (Continuum Surelite II-10). Helium gas with ~4 atm backing pressure was allowed to expand through a pulsed valve (General Valve Series 9) into the source to cool the formed clusters. The generated cluster anions were mass-analyzed with the TOF mass spectrometer. The $V_xSi_{12}^-$ (x=1, 2, 3) clusters were individually selected with a mass gate, decelerated by a momentum decelerator, and crossed with the beam of an

Nd:YAG laser (Continuum Surelite II-10, 266 nm) at the photodetachment region. The electrons from photodetachment were energy-analyzed by the magnetic bottle photoelectron spectrometer. The resolution of the photoelectron spectrometer is about ~40 meV for electrons with 1 eV kinetic energy.

To determine the lowest-energy structures of $V_xSi_{12}^-$ (x=1, 2, 3) clusters, we performed an unbiased global search using a genetic algorithm (GA)[44, 45] incorporated with DFT. The details of this GA-DFT scheme can be found in our previous publication[46]. For each cluster, sixteen random configurations were generated from scratch as the initial GA population. The GA search was continued for at least 1000 iterations to ensure the global minimum structure. *Ab initio* calculations were performed using the spin-polarized all-electron DFT as implemented in the DMol[3] program[47]. The generalized gradient approximation (GGA) with PBE parameterization[48] was adopted to describe the exchange-correlation interaction. A double numerical basis set including d-polarization functions (DND) was employed. Vibrational analyses were performed to ensure that the optimized structures are true minima on the potential energy surface.

By definition, VDE is the energy difference between the anion and the neutral cluster with the latter fixed at the anion geometry; and AEA is the energy difference between the anionic and neutral clusters in their optimized lowest-energy configurations. For all calculations, only the ground-state electron configurations were involved, and no excited state has been considered. All of the VDE and AEA values were computed by the difference of total energies from DFT calculations. Based on the energy levels of anionic clusters, photoelectron spectra were simulated using the generalized Koopmans' theorem (GKT), which has been described before[49]. In the simulated DOS spectra, the peak of each transition corresponds to the removal of an electron from a specific molecular orbital of the cluster anion. During the simulation, the relative energies of the orbitals (ΔE_n) were calculated by the equation: $\Delta E_n = E_{(HOMO-n)} - E_{HOMO}$, where $E_{(HOMO-n)}$ is the energy of the (HOMO-n) orbital from theoretical calculations, E_{HOMO} is the energy of the HOMO, and ΔE_n is the relative energies of the (HOMO-n) orbital with regard to the HOMO. We first set the peak associated with the HOMO to the position of calculated VDE of each isomer, and shifted the peaks of the deeper orbitals according to their relative energies compared to the HOMO.

It is suspected that conventional GGA with PBE parameterization might not be very reliable for describing transition-metal systems with spin polarization[50]. Hence, we have employed RPBE[51], M06-L[52], and M06 functionals[53] (which have been recommended for transition metals[54]) to compute the VDEs and to simulate the photoelectron spectra of the V_xSi_{12} cluster anions. The results are provided in Table S4 and Figure S4 of the Supporting Information, respectively. Clearly, all four functionals (PBE, RPBE, M06 and M06-L) are able to reasonably reproduce the experimental VDEs, with average deviation between 0.05 and 0.09 eV. With the same PBE functional, the choice of basis sets has only minor influence on the computed VDE values. Similar coincidences are found in the simulated photoelectron spectra by different methods (Figure S4). Therefore, the present choice of PBE/DND scheme is backed up by the other functionals and basis sets.

Acknowledgments

This work was supported by the National Natural Science Foundation of China (No. 11134005, 11304030, 21103202), the Fundamental Research Funds for the Central Universities of China (No. DUT14LK19), and the Knowledge Innovation Program of the Chinese Academy of Sciences (No. KJCX2-EW-H01). The authors thank Prof. Jun Li and Prof . Ling Jiang for valuable discussions

Notes and references

[1] *A Key Laboratory of Materials Modification by Laser, Ion and Electron Beams Dalian University of Technology, Ministry of Education, Dalian 116024, China;*
E-mail: zhaojj@dlut.edu.cn
[2] *A State Key Laboratory of Molecular Reaction Dynamics, Institute of Chemistry, Chinese Academy of Sciences, Beijing 100190 (China);*
E-mail: zhengwj@iccas.ac.cn
[3] *Beijing Computational Science Research Center, Beijing 100089, China*
[4] *Department of Chemistry and Center for Computational Chemistry, University of Georgia, Athens, Georgia, USA*

† Electronic Supplementary Information (ESI) available: Cartesian coordinates, on-site charge, spin, and bond lengths, plots of low-energy isomer structures for $V_xSi_{12}^-$ (x=1, 2, 3) clusters. Spatial distribution of molecular orbitals for VSi_{12}^- cluster, energies of molecular orbitals for V_3Si_{12} and $V_3Si_{12}^-$ clusters. Comparison of VDEs and photoelectron spectra simulated by PBE, RPBE, M06, M06-L functionals and experiments. See DOI: 10.1039/b000000x/

1. V. Kumar, *Nanosilicon*, Elsevier, 2011.
2. X. Zhu and X. C. Zeng, *J. Chem. Phys.*, 2003, **118**, 3558.
3. X. L. Zhu, X. C. Zeng, Y. A. Lei and B. Pan, *J. Chem. Phys.*, 2004, **120**, 8985.
4. S. Yoo and X. C. Zeng, *J. Chem. Phys.*, 2006, **124**, 054304.
5. S. Yoo, J. Zhao, J. Wang and X. C. Zeng, *J. Am. Chem. Soc.*, 2004, **126**, 13845-13849.
6. H. Hiura, T. Miyazaki and T. Kanayama, *Phys. Rev. Lett.*, 2001, **86**, 1733-1736.
7. Y. Gao and X. C. Zeng, *J. Chem. Phys.*, 2005, **123**, 204325.
8. V. Kumar and Y. Kawazoe, *Phys. Rev. Lett.*, 2001, **87**, 045503.
9. V. T. Ngan, E. Janssens, P. Claes, J. T. Lyon, A. Fielicke, M. T. Nguyen and P. Lievens, *Chem.-Eur. J.*, 2012, **18**, 15788-15793.
10. J. He, K. Wu, R. Sa, Q. Li and Y. Wei, *Chem. Phys. Lett.*, 2010, **490**, 132-137.
11. V. Kumar, *Comput. Mater. Sci.*, 2006, **36**, 1-11.
12. H.-G. Xu, X.-Y. Kong, X.-J. Deng, Z.-G. Zhang and W.-J. Zheng, *J. Chem. Phys.*, 2014, **140**, 024308.
13. A. K. Singh, T. M. Briere, V. Kumar and Y. Kawazoe, *Phys. Rev. Lett.*, 2003, **91**, 146802.
14. N. A. Antonis, M. Giannis, E. F. George and M. Madhu, *New J. Phys.*, 2002, **4**, 78.
15. L. Ma, J. Zhao, J. Wang, B. Wang, Q. Lu and G. Wang, *Phys. Rev. B*, 2006, **73**, 125439.
16. J. Wang, J. Zhao, L. Ma, G. Wang and R. B. King, *Nanotechnology*, 2007, **18**, 235705.
17. S. N. Khanna, B. K. Rao and P. Jena, *Phys. Rev. Lett.*, 2002, **89**, 016803.
18. J. U. Reveles and S. Khanna, *Phys. Rev. B*, 2005, **72**, 165413.
19. N. Uchida, T. Miyazaki and T. Kanayama, *Phys. Rev. B*, 2006, **74**, 205427.

20. J. Lu and S. Nagase, *Phys. Rev. Lett.*, 2003, **90**, 115506.
21. W. J. Zheng, J. M. Nilles, D. Radisic and K. H. Bowen, *J. Chem. Phys.*, 2005, **122**, 071101.
22. X. Y. Kong, H.-G. Xu and W. J. Zheng, *J. Chem. Phys.*, 2012, **137**, 064307.
23. H.-G. Xu, M. M. Wu, Z.-G. Zhang, J.-Y. Yuan, Q. Sun and W.-J. Zheng, *J. Chem. Phys.*, 2012, **136**, 104308.
24. I. Langmuir, *Science*, 1921, **54**, 59-67.
25. P. Pyykkö, *J. Organomet. Chem.*, 2006, **691**, 4336-4340.
26. P. Sen and L. Mitas, *Phys. Rev. B*, 2003, **68**, 155404.
27. W. Ji and C. Luo, *Int. J. Quantum Chem*, 2012, **112**, 2525-2531.
28. V. Kumar and Y. Kawazoe, *Phys. Rev. Lett.*, 2003, **90**, 055502.
29. H.-G. Xu, Z.-G. Zhang, Y. Feng, J. Yuan, Y. Zhao and W. Zheng, *Chem. Phys. Lett.*, 2010, **487**, 204-208.
30. H.-G. Xu, Z.-G. Zhang, Y. Feng and W. Zheng, *Chem. Phys. Lett.*, 2010, **498**, 22-26.
31. P. Claes, E. Janssens, V. T. Ngan, P. Gruene, J. T. Lyon, D. J. Harding, A. Fielicke, M. T. Nguyen and P. Lievens, *Phys. Rev. Lett.*, 2011, **107**, 173401.
32. K. Wade, *Chem. Soc. D*, 1971, 792-793.
33. D. M. P. Mingos, *Acc. Chem. Res.*, 1984, **17**, 311-319.
34. R. King, I. Silaghi-Dumitrescu and M. Uţă, *J. Chem. Theory Comput.*, 2008, **4**, 209-215.
35. F. Liu, M. R. Press, S. N. Khanna and P. Jena, *Phys. Rev. B*, 1989, **39**, 6914-6924.
36. A. Kirilyuk, A. Fielicke, K. Demyk, G. von Helden, G. Meijer and T. Rasing, *Phys. Rev. B*, 2010, **82**, 020405.
37. K. S. Williams, J. P. Hooper, J. M. Horn, J. M. Lightstone, H. Wang, Y. J. Ko and K. H. Bowen, *J. Chem. Phys.*, 2012, **136**, 134315.
38. C. Felser and G. H. Fecher, *Spintronics: From Materials to Devices*, Springer, 2013.
39. J. S. Moodera, T. S. Santos and T. Nagahama, *J. Phys.: Condens. Matter*, 2007, **19**, 165202.
40. F. Radu, R. Abrudan, I. Radu, D. Schmitz and H. Zabel, *Nat. Commun.*, 2012, **3**, 715.
41. L. Fang, K. D. Bozdag, C.-Y. Chen, P. Truitt, A. Epstein and E. Johnston-Halperin, *Phys. Rev. Lett.*, 2011, **106**, 156602.
42. F. Liu, M. Mostoller, T. Kaplan, S. N. Khanna and P. Jena, *Chem. Phys. Lett.*, 1996, **248**, 213.
43. C. Ashman, S. N. Khanna, F. Liu, P. Jena, T. Kaplan and M. Mostoller, *Phys. Rev. B*, 1997, **55**, 15868.
44. R. L. Johnston, *Dalton Trans.*, 2003, 4193-4207.
45. J. Zhao and R.-H. Xie, *J. Comput. Theor. Nanosci.*, 2004, **1**, 117-131.
46. L. Sai, L. Tang, J. Zhao, J. Wang and V. Kumar, *J. Chem. Phys.*, 2011, **135**, 184305.
47. B. Delley, *J. Chem. Phys.*, 2000, **113**, 7756-7764.
48. J. P. Perdew, K. Burke and M. Ernzerhof, *Phys. Rev. Lett.*, 1996, **77**, 3865.
49. J. Akola, M. Manninen, H. Häkkinen, U. Landman, X. Li and L.-S. Wang, *Phys. Rev. B*, 1999, **60**, R11297.
50. A. J. Cohen, P. Mori-Sanchez and W. Yang, *Science*, 2008, **321**, 792-794.
51. B. Hammer, L. B. Hansen and J. K. Nørskov, *Phys. Rev. B*, 1999, **59**, 7413-7421.
52. Y. Zhao and D. G. Truhlar, *J. Chem. Phys.*, 2006, **125**, 194101.
53. Y. Zhao and D. G. Truhlar, *Theor. Chem. Acc.*, 2008, **120**, 215-241.
54. S. Luo, B. Averkiev, K. R. Yang, X. Xu and D. G. Truhlar, *J. Chem. Theory Comput.*, 2014, **10**, 102.